© 2016. Published by The Company of Biologists Ltd | Journal of Experimental Biology (2016) 219, 2693-2703 doi:10.1242/jeb.137059

RESEARCH ARTICLE

Shoulder girdle rotation, forelimb movement and the influence of carapace shape on locomotion in *Testudo hermanni* (Testudinidae)

Manuela Schmidt*, Martin Mehlhorn and Martin S. Fischer

ABSTRACT

Studies into the function of structures are crucial for making connections between morphology and behaviour of organisms, but are still rare for the terrestrial Testudinidae. We investigated the kinematics of shoulder girdle and forelimb motion in Hermann's tortoise *Testudo hermanni* using biplanar X-ray fluoroscopy with a twofold aim: firstly, to understand how the derived shapes of shoulder girdle and carapace together influence rotation of the girdle; and, secondly, to understand how girdle rotation affects forelimb excursion. The total degree of shoulder rotation in the horizontal plane is similar to a species with a less domed shell, but because of the long and nearly vertically oriented scapular prong, shoulder girdle rotation contributes more than 30% to the horizontal arc of the humerus and nearly 40% to the rotational component of step length. The antebrachium and manus, which act as a functional unit, contribute roughly 50% to this component of the step length because of their large excursion almost parallel to the mid-sagittal plane. This large excursion is the result of the complex interplay between humerus long-axis rotation, counter-rotation of the antebrachium, and elbow flexion and extension. A significant proportion of forelimb step length results from body translation that is due to the propulsive effect of the other limbs during their stance phases. Traits that are similar to other tortoises and terrestrial or semi-aquatic turtles are the overall slow walk because of a low stride frequency, and the lateral-sequence, diagonally coupled footfall pattern with high duty factors. Intraspecific variation of carapace shape and shoulder girdle dimensions has a corresponding effect on forelimb kinematics.

KEY WORDS: Testudines, Terrestrial locomotion, Spatio-temporal gait parameters, Forelimb kinematics, Shoulder girdle morphology

INTRODUCTION

The unique morphology of Testudines has attracted the interest of morphologists for many decades, as they seek to answer questions about the evolutionary history of this clade, its relationship to other amniotes, and the relationship between morphology, behaviour and environment. Among amniotes, the clade Testudines is characterised by a number of derived character complexes, most of which concern the respiratory and the locomotor systems and are related to the evolutionary acquisition of a protective shell in the stem lineage of the clade (Romer, 1956; Zug, 1971; Walker, 1973; Burke, 1989; Joyce and Gauthier, 2004; Kuratani et al., 2011; Schoch and Sues, 2015). The vertebral column and ribs are incorporated into the dorsal carapace: their musculature is reduced and the trunk is immobile and rigid (Fig. 1A). The shell encloses the shoulder girdle and pelvis, and the points of insertion for several extrinsic limb muscles have changed accordingly (Walker, 1973; Nagashima et al., 2009). The triradiate shoulder girdle is unique in its shape among tetrapods. It comprises the scapulocoracoid (with a long, rod-shaped scapular prong projecting dorsally), a relatively long, rod-shaped acromion (projecting anteriorly) and a coracoid plate (projecting posteriorly). The scapular prong and acromion form a single osseous element, which articulates with the internal surface of the shell. The carapace and plastron are connected by lateral shell bridges, which leave an anterior and a posterior notch through which the body appendages can be withdrawn or extended.

The derived morphological characters of turtles have fundamental consequences for several biological functions, particularly with regards to locomotion and respiration (Friant, 1961; Gans and Hughes, 1967; Zug, 1971; Walker, 1973; Rivera et al., 2006; Landberg et al., 2003, 2009). Variation in size and shape of the shell within the Testudines has been demonstrated to significantly influence the volume of the lungs, the shape of the shoulder girdle and the excursion range of the limbs (Zug, 1971; Jayes and Alexander, 1980; Depecker et al., 2006a). It has even been suggested that, for terrestrial species, shell variation plays a role in thermoregulation and water conservation (Boyer, 1965). Statistically, a terrestrial mode of life correlates with a cupuliform carapace and an aquatic mode of life correlates with a flat shell (Claude et al., 2003). On the species level, however, we can find turtles with domed shells in aquatic environments and tortoises with very flat shells in terrestrial environments. Obviously, it is not only the physical environment but also the specific habitat that determines the selective forces acting on these structures and their functions. From this point of view, the question as to which selective factors determine the shape of the carapace has still not fully been answered, but it is of great importance when we attempt to outline the set of constraints that affect locomotion, respiration, reproduction and other biological functions. So far, our understanding is that a flat discoid or heart-shaped carapace is, for hydrodynamic reasons, advantageous in pelagic turtles, and that a cupuliform carapace is, for respiratory and/or osmoregulatory reasons, advantageous for land-dwelling turtles (Schubert-Soldern, 1962; Boyer, 1965; Patterson, 1973; Claude et al., 2003).

For locomotor performance on land, a domed and heavy carapace appears to be rather cumbersome. It prevents a number of basic terrestrial locomotor principles used by other groups of amniotes, such as the lateral bending of the trunk, extensive limb excursions, and variability in footfall sequences and gaits in order to achieve

Institute of Systematic Zoology and Evolutionary Biology, Friedrich-Schiller-University Jena, Erbertstraße 1, Jena 07743, Germany.

*Author for correspondence (schmidt.manuela@uni-jena.de)

M.S., 0000-0002-5931-8596

Received 1 January 2016; Accepted 20 June 2016

Journal of Experimental Biology (2016) 219, 2693-2703 doi:10.1242/jeb.137059

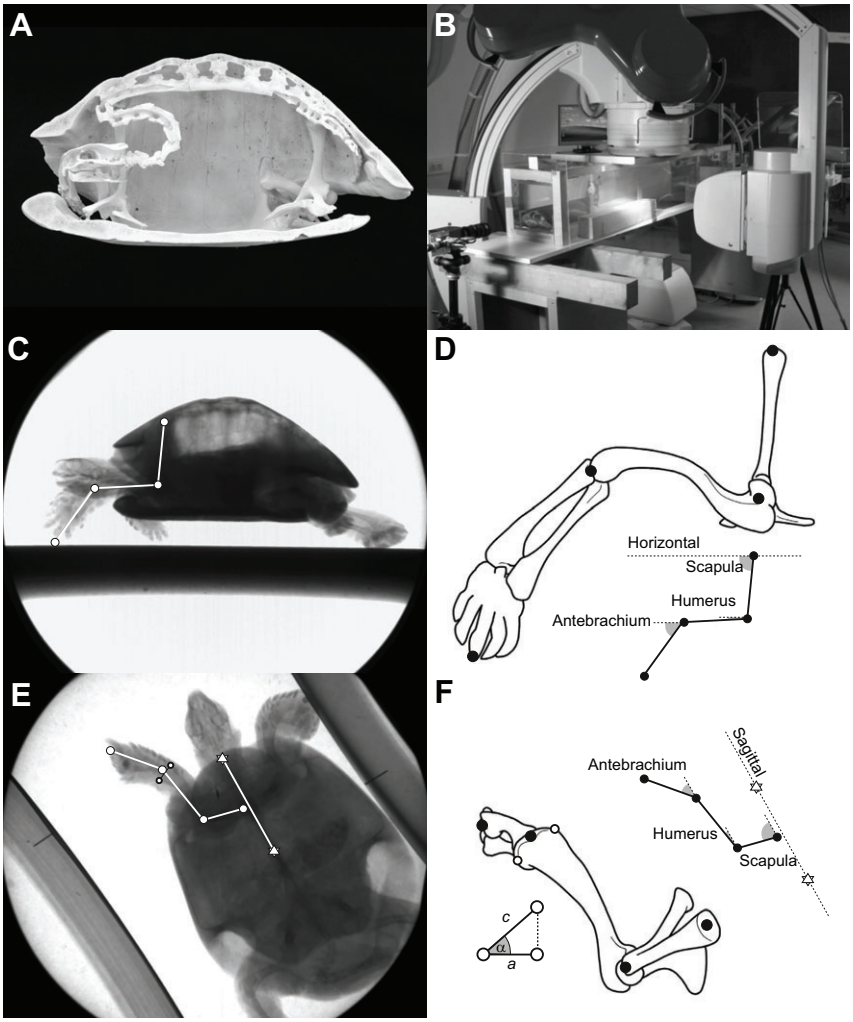

Fig. 1. Skeletal morphology, experimental setup, data acquisition and parameter description. (A) Skeletal preparation of a specimen of *Testudo hermanni* transected in the mid-sagittal plane illustrates the position of limb girdles within the shell. (B) Walking track integrated into the biplanar C-arm fluoroscope. (C) X-ray radiograph of a walking tortoise in lateral perspective showing tracked landmarks. (D) Landmark position projected onto the shoulder girdle and forelimb skeleton; definition of angles in lateral perspective. (E) X-ray radiograph in ventrodorsal perspective showing tracked landmarks. (F) Landmark position projected onto the skeleton; definition of angles in horizontal perspective. Estimation of humerus long-axis rotation: *c*, maximum projected distance between the landmarks; *a*, minimum projected distance; $\cos\alpha = a/c$, maximum long-axis rotation.

dynamic stability of the body in motion (Gray, 1944; Zug, 1971; Jayes and Alexander, 1980; Hildebrand, 1985; Zani et al., 2005). On land, turtles are slow walkers and appear rather clumsy in their overall performance. Agility and manoeuvrability are limited by the weight of the shell, and by the structural and physiological properties of the muscles, which limit the speed of contraction, as has been shown for *Testudo graeca* and *Testudo hermanni* (Woledge, 1968).

The adaptive values of several other derived characters in the locomotor system of terrestrial turtles, e.g. the shape of shoulder girdle and limb elements, their proportions, and the function of extrinsic and intrinsic limb muscles, still remain widely enigmatic. One reason for this is the relatively small number of biomechanical or physiological studies of terrestrial locomotion. Kinematic, kinetic and electrophysiological examinations are technically challenging because of the massive shell and the thick osteoderms covering the distal parts of the limbs. These protective structures impede an accurate description of limb movements, not to mention the challenges they pose in recording muscle activity. Even the measurement of substrate reaction forces can be complicated by the long contact times of the limbs.

Some of these challenges can be met by using X-ray fluoroscopy to demonstrate the kinematics of the skeletal elements within the shell and beneath the thick skin. More than 40 years ago, Warren F. Walker (1971) published the first, and to our knowledge the sole, X-ray-based analysis of forelimb and hindlimb kinematics in a walking turtle – the semi-aquatic painted turtle *Chrysemys picta* (Emydidae). For the first time, he was able to quantify the degree of shoulder girdle rotation and its contribution to the excursion of the humerus, even though the potential effect of girdle motion had been suggested long before (Ogushi, 1911).

The purpose of our study is to investigate the shoulder girdle and forelimb kinematics during terrestrial locomotion in another species, the Hermann's tortoise *Testudo hermanni*, which belongs to the clade Testudinidae and lives in a different habitat to the painted turtle *Chrysemys*. Free-living *T. hermanni* are widespread in southern Europe, including the Mediterranean isles, where the animals inhabit forests with a dense scrub layer growing in chalky soil, and also sand hills with halophilic vegetation (Fritz, 2001). Compared with the semi-aquatic *Chrysemys*, the Hermann's tortoise exhibits different body and limb proportions. We are able to test how these morphological differences influence the movement of the forelimb and the shoulder. We quantified shoulder girdle rotation and forelimb kinematics from biplanar X-ray fluoroscopic recordings taken while the animals moved along a horizontal track. Footfall patterns and spatiotemporal gait parameters were documented in order to characterise the locomotor performance of the animals and its speed-dependent variation. By comparing our findings with the functional properties of walking in other terrestrial turtles, we attempt to identify principles of locomotion that are used to maximise performance within the inherent framework of structural and physiological constraints of Testudines.

Journal of Experimental Biology

Journal of Experimental Biology (2016) 219, 2693-2703 doi:10.1242/jeb.137059

MATERIALS AND METHODS

Animals

Three adult tortoises (*Testudo hermanni* Gmelin 1789), two females and one male, weighing between 954 and 2318 g were kindly provided by the Zoo-park Erfurt, Thüringen. For the duration of the experiments, the animals were kept in spacious terrariums in our laboratory, where they were exposed to ambient light patterns. They were fed a diet of various fresh herbs; water was available *ad libitum*. The animals were looked after in accordance with German animal welfare regulations, and experimental procedures were registered with the Thuringian Committee for Animal Research (02-038/10).

Prior to the experiments, the animals were weighed and their carapaces were measured. We took the maximum linear dimensions in length, height and width. These so-called straight-line standard lengths omit the curvature of the carapace. Later, from the biplanar X-ray radiographs, we determined the lengths of the shoulder girdle and forelimb elements of each individual (Table 1).

Experimental setup and data collection

Our experimental setup consisted of a wooden track, on which the animals moved within a transparent Plexiglas enclosure (Fig. 1B). The surface of the track was covered with a thin sheet of foam rubber to provide traction. The enclosure kept the animals on an almost straight path while they passed the recording fields of the cameras. By holding a lettuce leaf tied to a string in front of the animals, they were encouraged to move forwards. An infrared heat source was placed at the end of the track to further motivate the animals to move. Out of our subjects, the two smaller tortoises were very cooperative and often displayed continuous periods of movement, while the larger tortoise (Testudo 1) often paused along the track.

High-resolution videoradiography was used to collect data on shoulder girdle and forelimb kinematics synchronously in lateral and ventrodorsal projection (Fig. 1C,E). Our biplanar C-arm fluoroscope (Neurostar, Siemens AG, Erlangen, Germany) operates with high-speed cameras (SpeedCam Visario G2, Weinberger GmbH, Erlangen, Germany) and a maximum spatial resolution of 1536×1024 dpi. For the purposes of this study, a frame frequency of 250 Hz was used. Two normal-light cameras (SpeedCam MiniVis) operating at the same frequency and synchronised to the X-ray fluoroscope were used to document the entire trial from frontal and lateral perspectives.

For the large female subject, it was not possible to depict both the shoulder girdle and the forefoot movements in the same recordings using the same X-ray dosage in lateral perspective. This was due to the large difference in electron density of the body parts inside and outside the shell. Therefore, we optimised the dosage for depicting the movements within the shell for this individual by combining 'softer' radiation with higher current intensity (lateral: 60 kV, 100 mA; ventrodorsal: 45 kV, 85 mA). Such limitations were not a factor for the smaller individuals (lateral: 75 kV, 40–100 mA; ventrodorsal: 75 kV, 40–100 mA). Contrast and sharpness were post-processed to improve visibility of the structures of interest using the camera-controlling software (Visart 3.2, High-Speed Vision, Karlsruhe, Germany). The distortion of the X-ray radiographs was corrected using a MATLAB routine based on a recorded grid (Brainerd et al., 2010). For the spatial calibration of the biplanar X-ray radiographs, we used a 3D grid made of an acryl cuboid, which has small steel spheres (Ø=1.5 mm) implanted on each surface at a distance of 10 mm in each direction.

Spatiotemporal parameters of forelimb excursion and the kinematics of the shoulder girdle and forelimb elements were quantified by manually tracking skeletal landmarks at the proximal and distal ends of the long bones using SimiMotion 3D (Simi Reality Motion Systems, Unterschleissheim, Germany) in both the lateral and the ventrodorsal projections (Fig. 1C–F). The landmarks were chosen so that their connecting lines best represent the functional long axes of the limb elements. Shoulder girdle rotation was quantified by the angular excursion of the scapular prong relative to the horizontal and to the mid-sagittal plane. Unfortunately, we were not allowed to implant radio-opaque markers into the loaned animals, which made it extremely difficult to identify exactly the same landmarks in both perspectives. To validate landmark identification, we repeated the tracking of the landmarks for a selected sequence five times and compared the quantified angles. The obtained measurement error was lowest for segment angles (maximum deviation: 2–5 deg), but added up to relatively large errors for 3-D joint angles (>10 deg). Because of the probability that this measurement error exceeds the natural variation across the stride cycles of an animal, we focus our kinematic analysis on the limb elements and omit the quantification of joint angles. The movements of limb elements were projected onto the sagittal and the horizontal planes, respectively, because these projected angles allowed us to differentiate between the amount of protraction–retraction and abduction–adduction of each element. We estimated the long-axis rotation of the humerus by quantifying the width of the bone shaft near the elbow joint from the X-ray radiographs in ventrodorsal projection (Fig. 1F). The maximum measurement of this distance (=*c*) indicates that the anatomical ventral surface of the humerus is directed to the ground. Long-axis rotation induces a shortening of the projected distance (=*a*). The angle of rotation (α) is then calculated using the formula: $\cos\alpha = a/c$. However, because the cosine function produces a systematic error in estimating the linear increment of angles from 0 to 90 deg if the cosine of the angle approaches one of the vertices of the cosine wave, we evaluated the accuracy of measurements using a forelimb skeleton mounted on a mini-tripod. We rotated the platform stepwise to compare the real angle of humerus long axis (obtained from the platform angle in frontal radiographs) with the trigonometrically determined angle from ventrodorsal radiographs at various positions (Fig. S1). We found that in the range of 35 to 55 deg, the accuracy of measurement is quite acceptable. Here, only the error of landmark tracking causes deviations of the computed angle from the real angle. Tracking error ranged between 0.2 and 1.5 mm for the distance between distal condyles of the humerus and caused a maximum error of ±7 deg for the estimated angle.

Table 1. Body mass and linear dimensions of carapace, shoulder girdle and forelimb elements

	Testudo 1 (female)	Testudo 2 (male)	Testudo 3 (female)
Body mass (g)	2318	954	1170
Carapace (mm)			
Maximum length	218	161	173
Maximum width	172	130	135
Maximum height	98	85	83
Shoulder girdle (mm)			
Scapular prong	46	40	38
Acromion	29	21	24
Coracoid	29	21	24
Forelimb (mm)			
Humerus	52	39	41
Antebrachium+manus	44	41	36

Journal of Experimental Biology (2016) 219, 2693-2703 doi:10.1242/jeb.137059

Data analysis and statistics

Animal speed was obtained by tracking an anterior and a posterior landmark on the shell, ensuring that at least one landmark was always in the visible field. Speed was calculated as the distance one of these landmarks moved over time. From the timing of the forefoot placements and lift-offs, we quantified stride frequency, stance and swing duration as well as the duty factor (stance duration relative to stride duration). The distance covered by the body, e.g. the carapace landmark, during stance phase is defined as stance length, and the distance covered by the forefoot during swing phase is defined as swing length (synonymous with step length). We define 'stride length' as the distance that the body covers during one stride cycle. Raw data for these computations were captured from the X-ray radiographs in a ventrodorsal projection, and hence are available for all three individuals. Linear regression analyses were carried out to identify the speed-dependent portion of variation in spatiotemporal gait parameters. *F*-values were tested for significance, and the coefficient of determination r^2 was calculated.

In order to compare the speed ranges between the three tortoises, we converted animal speed into a dimensionless variable using the Froude number formula: $Fr=v/\boldsymbol{g}l_0$ (Alexander and Jayes, 1983), where v is raw speed, $\boldsymbol{g}$ is gravitational acceleration and l_0 is the cube root of body mass as characteristic linear dimension, which scales isometrically with body mass. Stride frequency and stride length were converted into dimensionless variables using the formulas by Hof (1996): dimensionless frequency$=f/\boldsymbol{g}l_0$, where f is raw frequency, and dimensionless stride length$=l/l_0$, where l is raw stride length.

RESULTS

A total of 34 trials of cyclic walking performance were obtained for the analysis of shoulder girdle and forelimb kinematics in the three tortoises. From these trials, we were able to collect spatiotemporal gait parameters for 40 complete stride cycles and a number of singular stance and swing phases. Walking speed ranged between 0.02 and 0.10 m s^{-1} in total, in which the large female, Testudo 1, walked at the lower limit of speed range (v=0.02–0.04 m s^{-1}, Fr=0.006–0.010) and the male, Testudo 2, at the highest speeds (v=0.04–0.10 m s^{-1}, Fr=0.012–0.032).

Footfall pattern and speed variation

Footfall pattern was invariant across all trials in all three individuals and can be characterised as a 'lateral sequence, diagonal couplets' pattern according to Hildebrand (1966) (Fig. 2). Duty factor, the relative duration of the stance phase, is generally high. It ranges between 56.8 and 87.1%. Normally, duty factor is a reliable estimate of relative animal velocity with high duty factors corresponding to slow walks and vice versa. In our sample, however, the slowest moving individual (Testudo 1) showed an average duty factor of 69.1±8.6% while the faster moving individuals walked with higher average duty factors of 77.9±3.8% (Testudo 2) and 77.4±6.4% (Testudo 3). The reason for this discrepancy was the overall low velocity of limb movement in the large individual: stance phase movement was not faster, but swing phase movement was much slower than in the other individuals, leading to this shift in the proportions of stride cycle phases.

The instantaneous forward velocity of the landmark on the carapace oscillates around the average speed of the stride cycle with maximum values coinciding with the placement of a hind foot (Fig. 2A). Maximum acceleration, therefore, falls together with the swing phase of the contralateral forelimb. Forward velocity falls to a minimum if a hind foot is placed on the ground initiating the

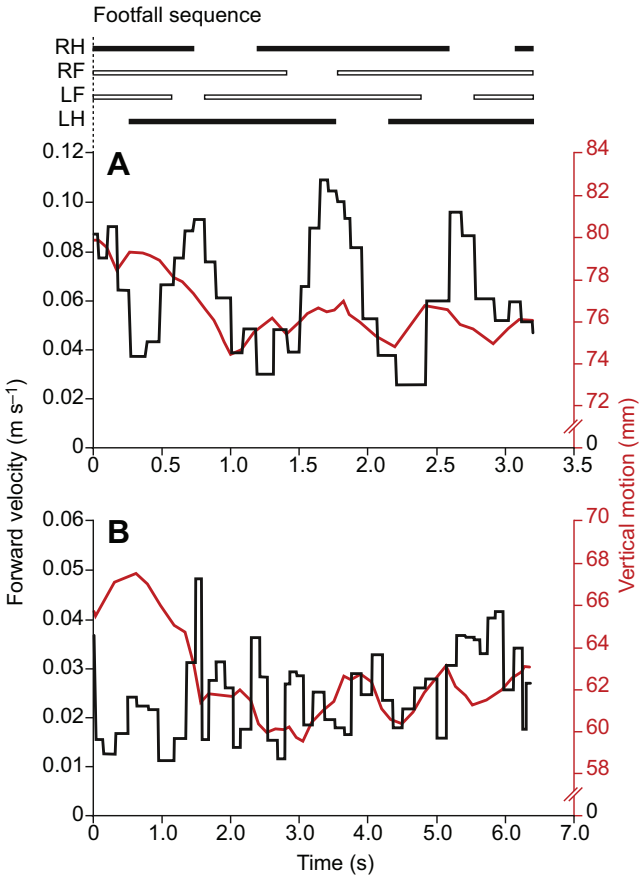

Fig. 2. Footfall sequence, oscillation of instantaneous forward velocity (black line, left *y*-axis) and vertical oscillation (red line, right *y*-axis) of the body. (A) Walking speed: 0.06 m s^{-1}; duty factor of the left forelimb: 83. (B) Walking speed: 0.03 m s^{-1}; duty factor of the left forelimb: 87. Each sequence starts with the footfall of the left forelimb (LF). RF, right forelimb; RH, right hindlimb; LH, left hindlimb.

quadrupedal phase of stance during the stride. At a slow walking speed, this regular oscillation is obscured and cannot be assigned to specific kinematic events within the cycle (Fig. 2B). Oscillations in the height of the body also occur, coinciding with oscillations of forward velocity except for the slow strides.

The tortoises change their walking speed primarily by changing temporal variables (Table 2). A decrease of stance phase duration and, to a lesser degree, of swing phase duration contributes to an increase of stride frequency and walking speed. Stride length and step length vary to a minor degree and the largest portion of this variation is random. Only in Testudo 1 does the speed-dependent variation of stride length and step length reach a significant level. Looking at the average values of the stride parameters, differences among the three individuals appear to concern both temporal and spatial parameters, with the male having higher stride frequencies and lower stance phase and swing phase durations than the females. There is hardly any overlap in the range of stride length and step length between the male and the females. However, for reliable comparison, we have to take differences in body size and speed range into account. Therefore, we converted speed, stride frequency and stride length into dimensionless variables. Fig. 3 shows the distribution of dimensionless frequency and dimensionless stride length across Froude number. The variables of the females fall together, and we pooled their data for computing the power formula to compare *y*-intercept and slope (±95% confidence interval) of the

Journal of Experimental Biology (2016) 219, 2693-2703 doi:10.1242/jeb.137059

Table 2. Spatio-temporal gait parameters

	Testudo 1	Testudo 2	Testudo 3
Stride frequency (s^{-1})			
Mean±s.d. (*n*)	0.25±0.03 (6)	0.48±0.14 (11)	0.32±0.07 (23)
Range	0.23–0.30	0.27–0.73	0.17–0.47
F-value/r^2	21.47**/84.1	86.78***/90.6	50.66***/70.7
Stride length (m)			
Mean±s.d. (*n*)	0.11±0.01 (6)	0.14±0.01 (11)	0.10±0.01 (23)
Range	0.09–0.12	0.12–0.17	0.07–0.13
F-value/r^2	9.42*/70.1	2.55/22.1	2.67/11.3
Stance duration (s)			
Mean±s.d. (*n*)	2.89±0.49 (13)	1.75±0.54 (35)	2.45±0.64 (38)
Range	2.23–3.82	1.05–3.37	1.15–4.86
F-value/r^2	10.10**/47.4	155.01***/82.4	57.67***/61.5
Swing duration (s)			
Mean±s.d. (*n*)	1.33±0.36 (12)	0.53±0.26 (20)	0.70±0.28 (37)
Range	0.80–1.88	0.26–1.42	0.41–1.50
F-value/r^2	0.93/8.5	12.38**/40.7	11.71**/25.1
Swing/step length (m)			
Mean±s.d. (*n*)	0.09±0.01 (12)	0.12±0.02 (20)	0.08±0.01 (37)
Range	0.06–0.11	0.10–0.16	0.05–0.11
F-value/r^2	7.23*/41.8	0.95/5.0	2.93/7.7

*P<0.05; **P<0.01; ***P<0.001.

regression lines between the genders. Contrary to indications from the average raw data, dimensionless frequency tends to be lower in the male (*y*-intercept: 0.018±0.033, slope: 6.02±1.46) than in the females (*y*-intercept: 0.033±0.019, slope: 7.08±1.86) when compared at equivalent speed (Fig. 3A). However, dimensionless stride length is significantly higher in the male (*y*-intercept: 0.125±0.029, slope: 0.90±1.29) than in the females (*y*-intercept: 0.069±0.017, slope: 2.68±1.67) (Fig. 3B). In the following section we describe shoulder girdle and forelimb movements in general and explore how differences in morphology and kinematics between the genders may contribute to the relative longer strides in the male individual.

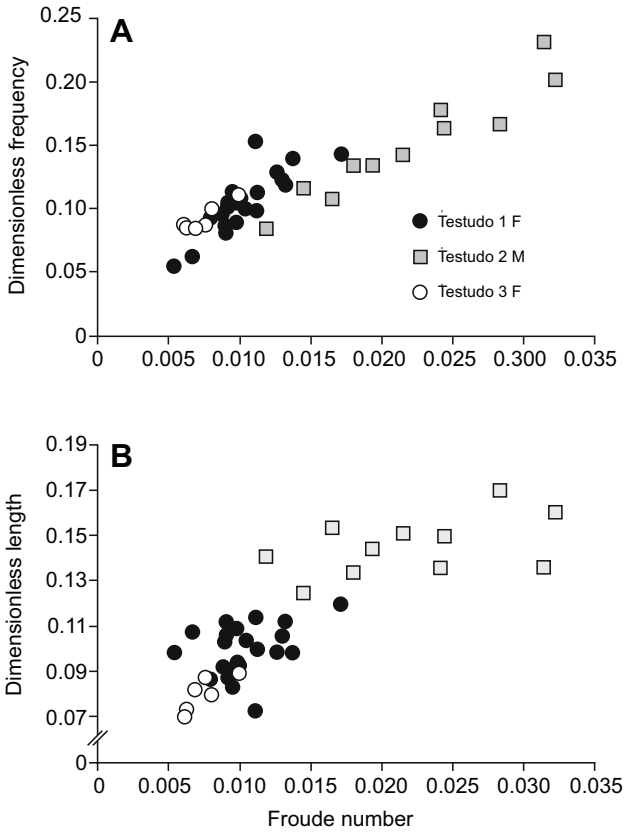

Fig. 3. Speed-related changes in the dimensionless gait parameters of the forelimb. (A) Stride frequency. (B) Stride length. Speed, frequency and length were transformed into dimensionless variables using formulas by Alexander and Jayes (1983) and Hof (1996).

Shoulder girdle shape and movement

The columnar scapular prong is the longest element of the triradiate shoulder girdle; the acromion and the blade-like coracoid are shorter and are always the same length in each of our tortoises (see Table 1). In the two females, their maximum length constituted 63% of the length of the scapular prong. The scapular prong of the male, however, is relatively longer because of the higher carapace, and the lengths of acromion and coracoid only constituted 53% of its length.

The scapular prong is connected to the anterior border of the first rib, lateral to the vertebral column. A connection between the left and right girdles does not exist (Fig. 4A). The coracoid blades, where forelimb retractor muscles originate, do not articulate with the plastron. The acromio-endoplastral joint lies within the same parasagittal plane, only slightly anterior to the dorsal scapulo-carapacial articulation. As a consequence, the line connecting the two joints – the axis of shoulder girdle rotation – is nearly parallel to the mid-sagittal and the vertical planes of the body. Thus, girdle rotation in this vertical hinge can most effectively contribute to the horizontal arc of forelimb excursion. Unlike the rotational axis of the shoulder girdle, the long axes of the scapular prong and the acromion are inclined toward the mid-sagittal plane. So, the glenoid lies in an effective distance from the axis of girdle rotation enhancing the effect of rotation on the horizontal translation of the glenoid.

The horizontal arc of girdle rotation was quantified by the angular changes of the scapular prong relative to the mid-sagittal plane (Fig. 4B). The girdle reaches its maximum cranial rotation shortly after foot placement. Then, it continuously rotates backwards until the last quarter of the stance phase (Fig. 4C). The first phase of cranial rotation is relatively slow and the angle of the scapular prong changes only slightly until midswing. Then, the angle rapidly decreases until the start of the stance phase (Fig. 4D). With respect to the orientation of the girdle and the amount of rotation, there are significant differences between the male and the females. The angle of the scapular prong relative to the longitudinal axis of the body is generally smaller in the females (maximum caudal rotation: 73±6 deg) than in the male (maximum caudal rotation: 99±5 deg). Also, the maximum range of motion is somewhat smaller in the females (12±4 deg) than in the male (17±5 deg). However, the contribution of shoulder girdle rotation to the horizontal arc of the humerus is similar in male and females during stance (male 36% versus females 34%), and even marginally higher in females during swing (male 36% versus females 38%). This is indicative of differences that are also present with respect to the range of humerus excursion in the horizontal plane (Fig. 4E,F).

Differences in girdle rotation affect both the range of motion and the kinematic profile of humerus rotation, especially during the stance phase. In the male, shoulder girdle and humerus caudal rotation are coupled as long as the girdle rotates backwards (10 to 80% of stance phase). Humerus rotation lasts slightly longer, but also stops prior to the end of the stance phase. In the females, however, a distinct caudal rotation of the humerus in the horizontal plane only takes place during the second half of the stance phase and does not reach the maximum values observed for the male (male 48±9 deg versus females 33±3 deg). The

Journal of Experimental Biology (2016) 219, 2693-2703 doi:10.1242/jeb.137059

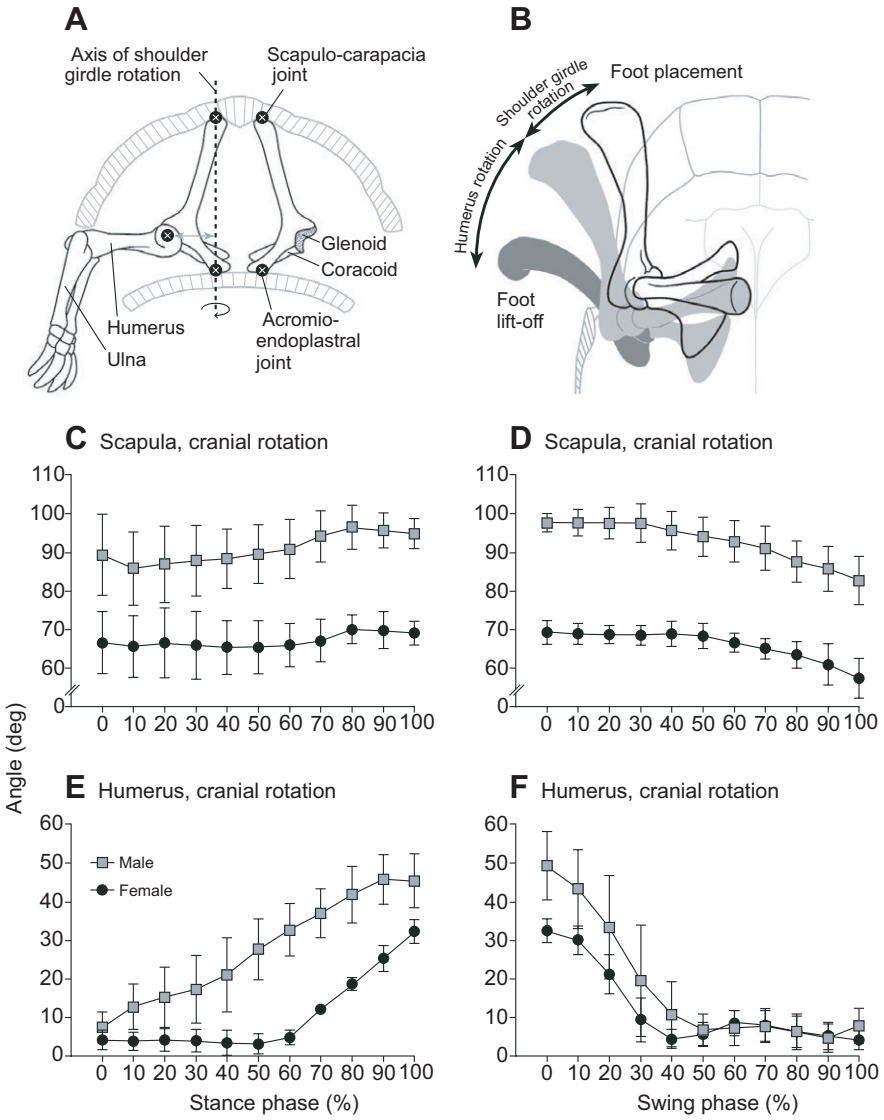

Fig. 4. Shoulder girdle and humerus rotation projected onto the horizontal plane. (A) Schematic cross-section through the anterior body illustrates the axis of girdle rotation. (B) Spatial contribution of girdle rotation to the total horizontal arc of the humerus from footfall to lift-off. (C,D) Caudal rotation (C) and cranial rotation (D) of the shoulder girdle. (E,F) Caudal rotation (E) and cranial rotation (F) of the humerus. Means and standard deviations were each computed from six stride cycles.

kinematic profiles of shoulder girdle and humerus cranial rotation during the swing phase are more similar in both genders, especially with respect to the remarkable decoupling of girdle rotation and humerus rotation. Forelimb protraction starts with a rapid flexion of the shoulder joint bringing the humerus close to its maximum cranial rotation angle, almost in parallel to the mid-sagittal plane. This position has already been reached by the middle of the swing phase. During the second half of the swing phase, girdle rotation pushes the protracted humerus even further towards the head, adding a remarkable translation component to the total excursion of the humerus.

We quantified the angle of the scapular prong to the horizontal in sagittal projection and found cranial inclinations of 76±4 deg in the females and 82±4 deg in the male at foot placement (Fig. 5A,B). During forelimb retraction, the angle of the scapular prong increases continuously in the male, but not in the females, where the caudal rotation occurs only during the second half of the stance phase. In its maximum retracted position, the scapular prong is nearly vertically oriented in the male (93±5 deg) and still cranially inclined in the females (81±5 deg). During forelimb protraction, the angle of the scapular prong relative to the horizontal decreases continuously in both the male and the females.

Forelimb shape and movement

The humerus of *T. hermanni* is the longest bone of the forelimb and its shaft is arched dorsally as in most other turtles and tortoises (Depecker et al., 2006b). The straight antebrachium is about half the length of the humerus. The carpus and metacarpus are short and broad, and appear to provide a high level of stability against intracarpal motion. Only the toes with their long claws are flexed during stance to accommodate the increasing load carried by the forelimb. The antebrachium and manus form a functional unit with no flexion–extension or abduction–adduction movements in the wrist joint.

The overall limb excursion angle, measured between the lines connecting the glenoid and the tip of the longest digit at foot placement and lift-off, ranges between 71 and 90 deg (mean: 80±7 deg) in the male. It shows much more variation in the female Testudo 3, for which this angle could be measured (range: 49–92 deg, mean: 71±14 deg). In general, the forelimb is much more protracted at foot placement (55±5 deg) than retracted at lift-off.

Looking at the excursions of the limb elements, we observe that the movement of the humerus occurs predominantly in the horizontal plane while the movements of the distal limb occur

Journal of Experimental Biology (2016) 219, 2693-2703 doi:10.1242/jeb.137059

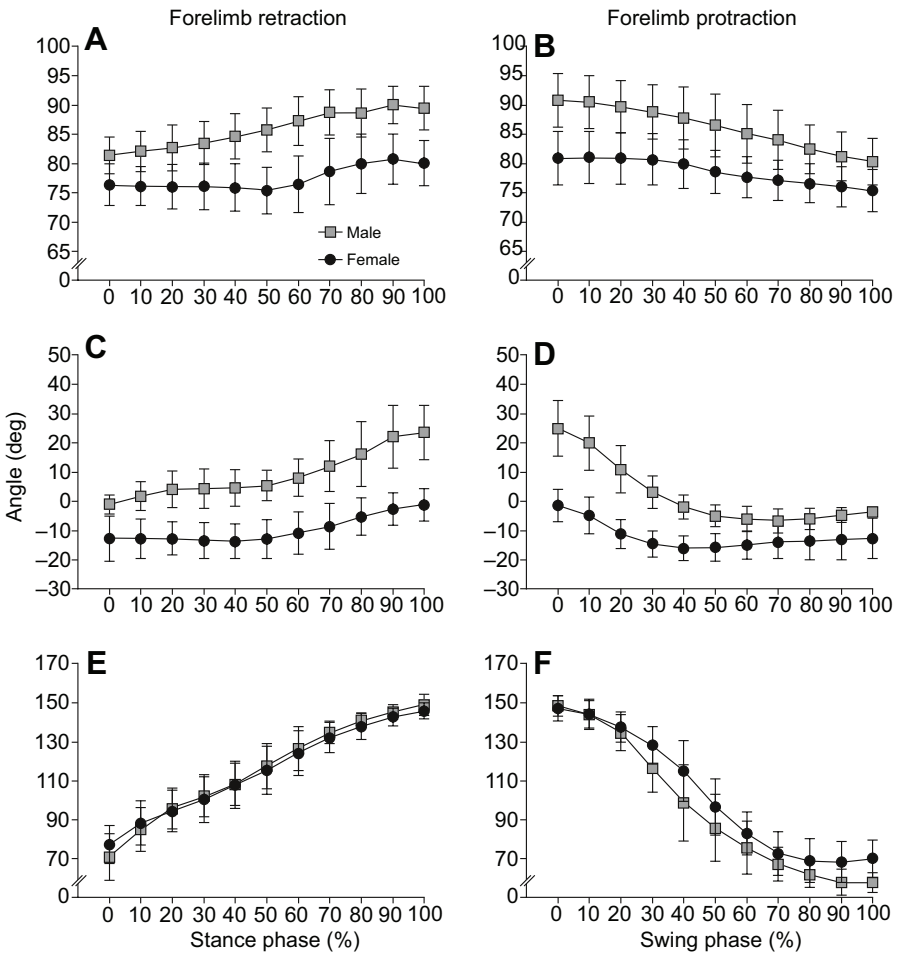

Fig. 5. Angular excursion during forelimb retraction and forelimb protraction, projected onto the sagittal plane. (A,B) Scapula; (C,D) humerus; (E,F) antebrachium and manus. Means and standard deviations were computed from six stride cycles in the male and nine stride cycles in the female.

predominantly in the vertical plane, hence a typical sprawled limb posture (Fig. 6). In their most protracted position, all limb elements are almost parallel to the sagittal plane. The distal end of the humerus is elevated approximately −13±7 deg above the horizontal in the females, but nearly parallel to the ground in the male (−2±2 deg) (Fig. 5C,D). The ventral surface of the humerus shaft faces towards the ground. During forelimb retraction, the humerus rotates caudally and becomes more and more abducted (Fig. 6). At the same time, the bone shaft rotates about its longitudinal axis, so that the ventral surface is directed posteriorly at foot lift-off. The main portion of this long axis rotation appears to result from humeral movements in the glenoid, but a smaller portion may be induced by changes in the glenoid height. We observed a small vertical shift of the glenoid cavity (4 to 6 mm), probably induced by the roll of the trunk from side to side. The distal end of the humerus is continuously lowered until the end of the stance phase, up to an average angle of 27±8 deg below the horizontal in the male. The humerus of the females is less depressed at foot lift-off (−1±5 deg). These differences in the humerus position relative to the horizontal mainly affect the effective length of the forelimb and its erectness, and they correspond to our observation that the male carries its shell higher above the ground than the females. Our estimates of long-axis rotation of the humerus for the male range between 38 and 47 deg (mean: 44±4 deg) and do not differ from those for the females, which range between 38 and 52 deg (mean: 44±5 deg).

The distal limb, the antebrachium and manus, shows the highest range of motion of all limb elements (Fig. 5E,F). At its most protracted position, the antebrachium is cranially inclined with the tip of the digits lying in front of the elbow joint (Fig. 6). The palmar surface of the foot and the plane, which intersects the radius and ulna of the antebrachium, both face laterally. The angle of the distal limb to the horizontal is on average 62±11 deg in the male and 74±10 deg in the small female. During limb retraction, the angle increases continuously until the end of the stance phase, when the distal limb is highly inclined to the horizontal (male: 149±5 deg, female: 147±13 deg), and the palm faces almost dorsally. With the increasing degree of humeral abduction, the elbow moves in a horizontal arch and the antebrachium becomes correspondingly adducted at the end of the stance phase. This effect apparently superimposes the abducting effect of the long-axis rotation of the humerus. Interestingly, the excursions of the distal limb are much more similar in male and female subjects than those of the humerus and shoulder girdle.

The high range of motion of the distal limb does not necessarily mean that this element contributes most to the step length of the limb. This is because the pivot height and the projected length of an element into the plane of forward movement are of equal or even greater relevance, as we will demonstrate in the following paragraphs.

Contribution of shoulder girdle and limb rotation to step length

Step length, the horizontal distance that the tip of the digit covers during the swing phase of the limb, is a composite of body translation (mainly achieved by the accelerating effect of the contralateral hindlimb) and rotation of the limb in swing (Fig. 7).

Journal of Experimental Biology (2016) 219, 2693-2703 doi:10.1242/jeb.137059

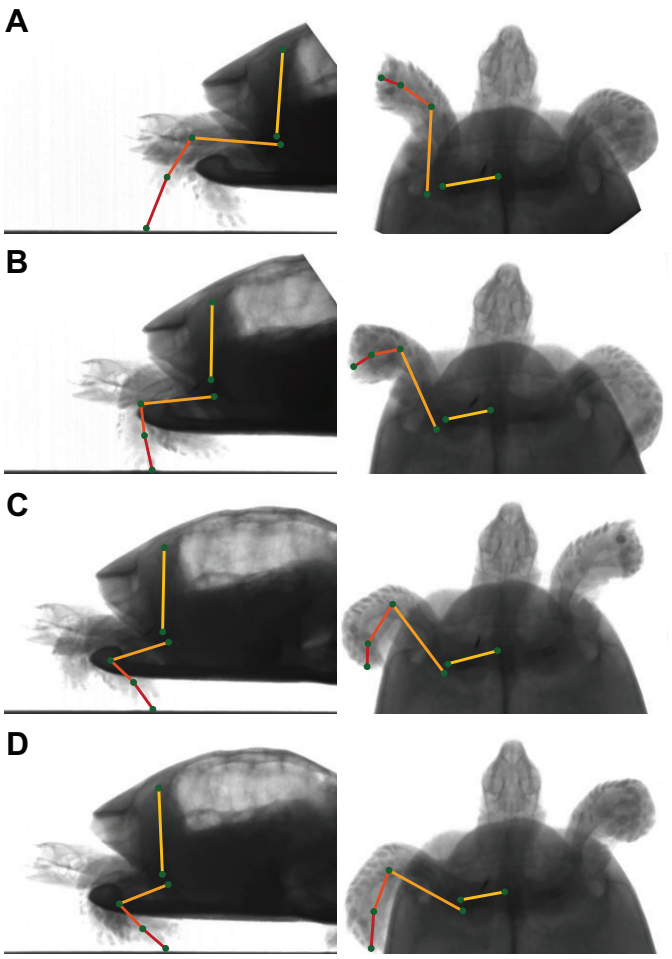

Fig. 6. Single-frame radiographs of Testudo 2 (male) in lateral (left) and ventrodorsal (right) projection. Excursion of the left forelimb during the stance phase. (A) Foot placement. (B) First third of stance phase. (C) Second third of stance phase. (D) Foot lift-off. The long axes of left limb elements are highlighted. The swing phase of the right forelimb lasts only from B to C.

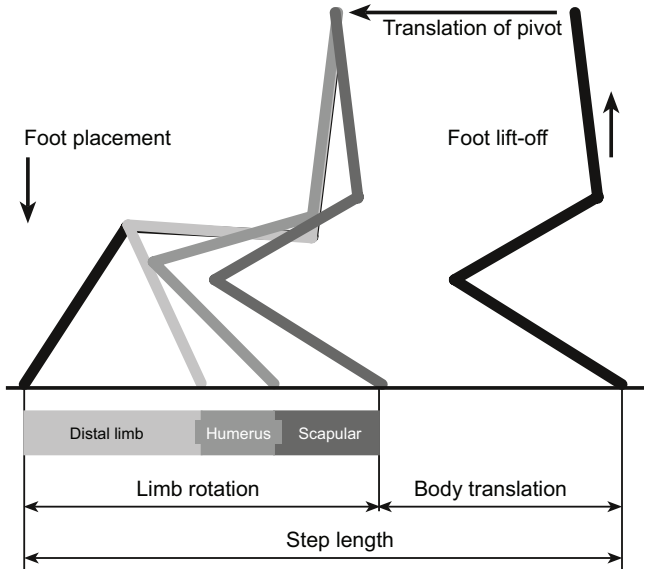

Fig. 7. Components of forelimb step length: body translation and limb rotation. The 'overlay method' (Fischer and Lehmann, 1998) enables the total rotation of the limb to be broken down into the proper rotation of each element and its contribution to the rotational component of the step length. Note that the illustrated rotation of the distal limb results not only from elbow extension but also from the long axis rotation of the humerus (see Results, 'Contribution of shoulder girdle and limb rotation to step length' for further explanation).

The relative amounts of rotation and translation can easily be quantified by measuring the horizontal translation of the most proximal joint (here, the scapulo-carapacial articulation) and subtracting this value from the measured step length. In our tortoises, the relative portion of body translation versus limb rotation on step length was on average 37:63 in the male and 28:72 in the female Testudo 3 (Table 3).

Using the so-called 'overlay method' proposed by Fischer and Lehmann (1998), the rotational component of step length can be further subdivided into the proportions that each rotating element contributes to the horizontal translation of the tip of the digit. The method is based on simple trigonometric computations using the angle of an element to the vertical plane (α) and its projected length (the hypotenuse of the right triangle) to calculate the length of the adjacent of the right triangle. This computation was carried out for the scapular prong, the humerus and the distal limb excursions during the swing phase frame by frame. Having these values, we subtract from the humerus excursion the part that results from scapular excursion and thus obtain the proper motion of the humerus in its proximal adjacent joint, the shoulder. Then, we subtract from the excursion of the antebrachium the part resulting from scapular and from humerus excursion and obtain the proper motion of the distal limb in the elbow joint. Finally, we compute the contribution of the proper motion of each element to the total rotational component of step length. However, a drawback of this method, originally developed for mammalian limbs, is that the proper motion of a single limb element cannot be further subdivided into the portion that results from flexion or extension of the proximal adjacent joint, and the portion that results from long-axis rotation of the proximal adjacent segment.

The results show that the contribution of distal limb excursion to step length is high but probably not as high as expected from its range of motion alone (Table 3). In the male, the proper motion of the distal limb by elbow extension (=opening of the caudal angle between humerus and antebrachium) combined with humerus long-axis rotation accounts for approximately 64% of its overall range of motion. The proper motion of the distal limb in the female Testudo 3 is remarkably higher, constituting approximately 83% of its overall range of motion, and consequently it contributes a higher portion to the amount of limb rotation than the distal limb of the male (61±6% versus 44±6%). The contribution of the humerus to step length appears very low by this method of computation, because of the apparently low degree of flexion and extension in the shoulder. In many cases, particularly in the female Testudo 3, the net joint

Table 3. Step length components and contribution of shoulder girdle and limb element rotation to the rotational component of step length

	Male (*n*=10)	Female (*n*=10)
Step length component (%)		
Body translation	36.9±3.5	28.3±7.5
Limb rotation	63.1±3.5	71.7±7.5
Contribution to the rotational component of step length (%)		
Scapular prong	39.9±7.8	36.3±11.4
Humerus	16.6±7.7	3.0±7.3
Antebrachium+manus	43.5±5.8	60.7±6.0
Proper motion of forelimb elements (% of total range of motion)		
Humerus	50.7±22.3	24.2±49.9
Antebrachium+manus	63.8±8.9	82.6±8.0

Journal of Experimental Biology

Journal of Experimental Biology (2016) 219, 2693-2703 doi:10.1242/jeb.137059

movement of the shoulder was directed against the overall forward direction of the limb swing (net joint extension instead of net joint flexion). In the male, however, we always observed a net joint flexion in the shoulder (=decrease of the cranial angle between scapular prong and humerus), and moreover, the pivot of humeral rotation was always held above the level of the elbow joint. In this way, the humerus can contribute more to the step length by its cranial rotation. Furthermore, when the contribution of long-axis rotation to the excursions of the antebrachium could be extracted, it should have added consequently to the overall humerus contribution. Shoulder girdle rotation contributes more than one-third to the rotational component of step length, and this high proportion results primarily from the high pivot position, not from a large angular excursion. So, even a relatively small range of motion in a high pivot can effectively facilitate the overall range of motion of the limb as a whole.

DISCUSSION

For *T. hermanni*, the act of walking on a flat horizontal track is characterised by a set of locomotor principles that has also been described for terrestrial locomotion in other tortoises and turtles: the slow speed combined with a lateral-sequence, diagonal-coupled footfall pattern and long periods of tripedal stance provide maximum static stability against pitching and rolling (Gray, 1944; Walker, 1971; Zug, 1971; Jayes and Alexander, 1980). Changes in walking speed result from changes in temporal (rather than spatial) gait parameters, in which both the swing phase duration and the stance phase duration decrease with increasing speed (Williams, 1981; Wren et al., 1998). Placement and angular excursion of limb elements vary randomly, but they are not dependent on the speed of locomotion.

With respect to limb kinematics, we found that the forelimbs are much more protracted than retracted during the course of the stride cycle. This reflects the limitation of the shell aperture on the excursion range of the limb (Walker, 1971; Zug, 1971). The degree of forelimb protraction is unusually high for tetrapods with sprawled limb postures and is facilitated by the morphology of the humerus, characterised by the arched shaft and the torsion of the distal shaft (approximately 90 deg) relative to the humeral head (Ogushi, 1911; Walker, 1971). Interestingly, humeral protraction at the beginning of the swing phase is quite fast in *T. hermanni* compared with other aspects of forelimb kinematics, and it is already completed by the middle of the swing phase, when the humerus is placed in parallel to the ground and in parallel to the sagittal plane of the body. In this position, even a small push by a relatively small amount of shoulder girdle cranial rotation has a substantial effect on forelimb protraction and forelimb step length. The long-axis rotation of the bone follows the same temporal pattern. It gradually increases during the stance phase and directs the antebrachium laterally. The counter-rotation, which starts immediately after foot lift-off and which spins the anatomical ventral surface back into the horizontal plane, is quickly terminated before mid-swing.

Walker (1971) estimated the increment of body forward progression added by the rotation of the shoulder girdle in a transverse plane of *C. picta* and found that it adds approximately 16 deg to the horizontal arc of humerus excursion, which corresponds to a portion of 27 to 32%. We obtained an excursion range of shoulder rotation in *T. hermanni* similar to that of the painted turtle, but its effect on forelimb step length is higher, ranging between 34 and 38% of the horizontal arc of the humerus excursion.

While this parameter is illustrative, it does not fully reflect the contribution of shoulder girdle rotation to the step length of the forelimb without considering the limb geometry in the sagittal projection. The pivot height of all joints and the differential contribution of proper motion versus passive transport of each limb element from the most distal to the most proximal one in the kinematic chain also have a significant impact on the step length of the forelimb. Their contribution can be more clearly demonstrated by estimating the effect of girdle rotation in sagittal projection (Fischer and Lehmann, 1998). In *T. hermanni*, we found that shoulder girdle rotation contributes more than 35% to the portion of step length, which results from limb rotation during swing. Although this parameter is not quantified for the painted turtle or for any other species of Testudines, we expect it would be lower in *C. picta*, reflecting the differences between the two species with respect to the shape and dimensions of the carapace and the shoulder girdle. Here, turtles with a cupuliform carapace and a relatively long and erect scapular prong have an advantage over species with a rather flat shell and inclined scapulae (Depecker et al., 2006a). So, despite not being primarily adaptive for terrestrial locomotion (Schubert-Soldern, 1962; Boyer, 1965; Patterson, 1973; Claude et al., 2003), the domed carapace of most of the Testudinidae and of the box turtles within Emydidae can compensate for some of the physiological constraints particular to terrestrial turtles, such as body weight and limb proportions.

Although each section is rather short and sturdy, the antebrachium and manus together contribute the most to the rotational component of step length, not only because of the high amount of proper motion in the elbow joint, but also because of the long-axis rotation of the humerus. Despite the remarkable outward-directed rotation of the humerus (up to 47 deg), the abduction angle of the antebrachium does not change to the same extent. It increases from approximately 25 deg at touchdown to approximately 40 deg at the end of the stance phase. This effect may result from the combination of elbow flexion and a counter-rotation of the antebrachium in the elbow joint, which we could not quantify but deduce from the changing direction of the palmar surface. The palm faces laterally at touchdown but posterodorsally at lift-off.

During the swing phase of a limb, the body moves forward by the propulsive effect of the other limbs on the ground. Hence, in addition to limb rotation during the swing phase, the translation of its proximal pivot because of the forward progression of the body contributes to the step length of a limb. We quantified the forward translation of the shoulder girdle during the swing phase and found that it contributes approximately one-third to the total step length of the forelimb. Gregory (1912) termed this component of step length the ‘acceleration increment’ and stated that its contribution to step length depends on the relationship between quadrupedal, tripedal and bipedal contact phases within a stride cycle. Its contribution to step length in *T. hermanni* appears relatively high given the predominance of quadrupedal and tripedal stance. However, our individuals, and some other turtles as well (Walker, 1971; Jayes and Alexander, 1980), are able to accelerate their body very quickly during the short bipedal phases of limb contact. The instantaneous velocity of the body then increases up to twice the average speed of the cycle. This acceleration apparently results from the pushing effect of the contralateral hindlimb at the end of its stance phase. As already described for other turtles (Walker, 1971; Zug, 1971), the far retracted hindlimb – together with the smaller transverse distance between the acetabula – results in a line of action closer to the sagittal plane. Deducing resultant forces from kinematics alone is speculative, but studies on substrate reaction forces exerted by turtles during terrestrial locomotion are very rare. Zani et al. (2005) illustrated the ground reaction forces for a walking trial in their study

on the giant Galápagos tortoise *Chelonoides nigra* (syn. *Geochelone elephantopus*). This tortoise carries most of its weight onto the forelimbs while the hindlimbs dominate in propulsion. In the smaller tortoise *Testudo graeca* and in *Geoemyda grandis*, peak vertical forces and vertical impulses exerted by the forelimbs and the hindlimbs, respectively, are nearly equal (Jayes and Alexander, 1980).

Coinciding the maximum propulsive power exerted by the hindlimb with the swing phase of the contralateral forelimb possibly allows the tortoise to compensate for the limited acceleration potential of the swinging limb visible in the long swing phase duration and is probably related to the slow contraction speed of tortoise muscles (Woledge, 1968). As extremely slow muscles generate force quite economically, the combination of a long tripedal stance with powerful body acceleration during the short bipedal phases appears to constitute a reliable mode of walking, probably less metabolically expensive than a faster walk with higher stride frequencies and lower duty factors (Baudinette et al., 2000). Zani and co-workers (Zani et al., 2005; Zani and Kram, 2008) present a similar argument in their findings on energy recovery mechanisms in the giant Galapagos tortoise and the ornate box turtle *Terrapene ornata*.

CONCLUSIONS

Our kinematic analysis of shoulder girdle and forelimb movements during walking in *T. hermanni* revealed some aspects that apparently support the locomotor performance in this species. The significant amount of power required to protract and retract the forelimbs is supplied by the extrinsic limb muscles, which rotate the shoulder girdle about a nearly vertical axis at an effective distance from the glenoid. Thus, a relatively small amount of excursion has a maximum effect on step length. This principle is probably applicable to turtles in general, but the shape of the carapace and its influence on the dimensions and orientation of the shoulder girdle within the shell enhance this effect considerably – as the differences among our individuals illustrate. The longer scapular prong allows the male to achieve a longer step and, even with a lower frequency compared with the females, it still achieves higher walking speeds. These effects were greater than anticipated, otherwise we would have increased our sample of individuals. Nevertheless, even a comparison on an individual level demonstrates how intraspecific variations in shape and structural dimensions may shift the range of variation in functional parameters, and in future studies, the influence of variation in skeletal elements on the mechanics of the locomotor apparatus will probably receive more attention. In this context, the low variation of spatial gait parameters in the two faster moving individuals is remarkable. It appears that only the large, very slow-walking female still had the potential to further increase step length (and thus speed), while the kinematics of the other individuals attained a limitation or the optimized limb geometry for maximal spatial excursion.

Acknowledgements

We wish to thank Rommy Petersohn for her competent assistance with the C-arm fluoroscope and for her patience and motivation during all experimental sessions. We thank the editor and two anonymous reviewers for their helpful suggestions on previous drafts of the manuscript. Animals were kindly provided by the Aquarium of the Thuringian Zoo, Erfurt. We thank Helen Johnson for her thoughtful editing of the language of the manuscript.

Competing interests

The authors declare no competing or financial interests.

Author contributions

M.S. and M.M. analyzed the data and interpreted the findings. M.S. wrote and revised the manuscript. M.M. executed the experiments and collected the data. M.S.F. designed the experiments, interpreted the findings, and revised the manuscript.

Funding

This research project was funded solely by the budget of the Institute of Systematic Zoology and Evolutionary Biology, Friedrich-Schiller-University Jena.

Data availability

All raw x-ray movies are available at the Jena Collection of X-ray Movies (http://szeb.thulb.uni-jena.de/szeb/templates/master/template_szeb/index.xml).

Supplementary information

Supplementary information available online at
http://jeb.biologists.org/lookup/doi/10.1242/jeb.137059.supplemental

References

Alexander, R. McN. and Jayes, A. S. (1983). A dynamic similarity hypothesis for the gaits of quadrupedal mammals. *J. Zool. Lond.* **201**, 135-152.
Baudinette, R. V., Miller, A. M. and Sarre, M. P. (2000). Aquatic and terrestrial locomotory energetics in a toad and a turtle: a search for generalisations among ectotherms. *Physiol. Biochem. Zool.* **73**, 672-682.
Boyer, D. R. (1965). Ecology of the basking habit in turtles. *Ecology* **46**, 99-113.
Brainerd, E. L., Baier, D. B., Gatesy, S. M., Hedrick, T. L., Metzger, K. A., Gilbert, S. L. and Crisco, J. J. (2010). X-ray reconstruction of moving morphology (XROMM): precision, accuracy and application in comparative biomechanics research. *J. Exp. Zool.* **313**, 262-279.
Burke, A. C. (1989). Development of the turtle carapace: implications for the evolution of a novel bauplan. *J. Morphol.* **199**, 363-378.
Claude, J., Paradis, E., Tong, H. and Auffray, J.-C. (2003). A geometric morphometric assessment of the effects of environment and cladogenesis on the evolution of the turtle shell. *Biol. J. Linn. Soc.* **79**, 485-501.
Depecker, M., Berge, C., Penin, X. and Renous, S. (2006a). Geometric morphometrics of the shoulder girdle in extant turtles (Chelonii). *J. Anat.* **208**, 35-45.
Depecker, M., Renous, S., Penin, X. and Berge, C. (2006b). Procrustes analysis: a tool to understand shape changes of the humerus in turtles (Chelonii). *C. R. Palevol.* **5**, 509-518.
Fischer, M. S. and Lehmann, R. (1998). Application of cineradiography for the metric and kinematic study of in-phase gaits during locomotion of the pika (*Ochotona rufescens*, Mammalia: Lagomorpha). *Zoology* **101**, 148-173.
Friant, M. (1961). Recherches sur la ceinture scapulaire des chéloniens. *Acta Anat.* **45**, 143-154.
Fritz, U. (2001). *Handbuch der Reptilien und Amphibien Europas. Band 3/IIIA: Schildkröten (Testudines) I*. Wiebelsheim: Aula-Verlag.
Gans, C. and Hughes, G. M. (1967). The mechanism of lung ventilation in the tortoise *Testudo graeca* (Linné). *J. Exp. Biol.* **47**, 1-20.
Gray, J. (1944). Studies in the mechanics of the tetrapod skeleton. *J. Exp. Biol.* **20**, 88-116.
Gregory, W. K. (1912). Notes on the principles of quadrupedal locomotion and on the mechanism of the limbs in hoofed animals. *Ann. N. Y. Acad. Sci.* **22**, 267-294.
Hildebrand, M. (1966). Analysis of the symmetrical gaits of tetrapods. *Folia Biotheor.* **6**, 9-22.
Hildebrand, M. (1985). Walking and running. In *Functional Vertebrate Morphology* (ed. M. Hildebrand, D. M. Bramble, K. F. Liem and D. B. Wake), pp. 38-57. Cambridge, MA: The Belknap Press of Harvard University Press.
Hof, A. L. (1996). Scaling gait data to body size. *Gait Posture* **4**, 222-223.
Jayes, A. S. and Alexander, R. McN. (1980). The gaits of chelonians: walking technique for very low speeds. *J. Zool. Lond.* **191**, 353-378.
Joyce, W. G. and Gauthier, J. A. (2004). Palaeoecology of Triassic stem turtles sheds new light on turtle origins. *Proc. R. Soc. Lond. B* **271**, 1-5.
Kuratani, S., Kuraku, S. and Nagashima, H. (2011). Evolutionary developmental perspective for the origin of turtles: the folding theory for the shell based on the developmental nature of the carapacial ridge. *Evol. Dev.* **13**, 1-14.
Landberg, T., Mailhot, J. D. and Brainerd, E. L. (2003). Lung ventilation during treadmill locomotion in a terrestrial turtle, *Terrapene carolina*. *J. Exp. Biol.* **206**, 3391-3404.
Landberg, T., Mailhot, J. D. and Brainerd, E. L. (2009). Lung ventilation during treadmill locomotion in a semi-aquatic turtle, *Trachemys scripta*. *J. Exp. Zool.* **311A**, 551-562.
Nagashima, H., Sugahara, F., Takechi, M., Ericsson, R., Kawashima-Ohya, Y., Narita, Y. and Kuratani, S. (2009). Evolution of the turtle body plan by the folding and creation of new muscle connections. *Science* **325**, 193-196.
Ogushi, K. (1911). Anatomische Studien an der japanischen dreikralligen Lippenschildkröte (*Trionyx japonicus*). I. Das Skeletsystem. *Morphol. Jahrbuch* **43**, 1-106.

Patterson, R. (1973). Why tortoises float. *J. Herpetol.* **7**, 373-375.
Rivera, G., Rivera, A. R. V., Dougherty, E. E. and Blob, R. W. (2006). Aquatic turning performance of painted turtles (*Chrysemys picta*) and functional consequences of a rigid body design. *J. Exp. Biol.* **209**, 4203-4213.
Romer, A. S. (1956). *Osteology of Reptiles*. Chicago, IL: University of Chicago Press.
Schoch, R. R. and Sues, H.-D. (2015). A Middle Triassic stem-turtle and the evolution of the turtle body plan. *Nature* **523**, 584-587.
Schubert-Soldern, R. (1962). Der Schildkrötenpanzer – Anpassung und Stammesentwicklung. *Verh. Zool. Botan. Gesell. Wien* **101-102**, 235-268.
Walker, W. F., Jr. (1971). A structural and functional analysis of walking in the turtle, *Chrysemys picta marginata*. *J. Morphol.* **134**, 195-214.
Walker, W. F., Jr. (1973). The locomotor apparatus of Testudines. In *Biology of the Reptilia, Vol. 4, Morphology D* (ed. C. Gans and T. S. Parsons), pp. 1-100. London: Academic Press.
Williams, T. L. (1981). Experimental analysis of the gait and frequency of locomotion in the tortoise, with a simple mathematical description. *J. Physiol.* **310**, 307-320.
Woledge, R. C. (1968). The energetics of tortoise muscle. *J. Physiol.* **197**, 685-707.
Wren, K., Claussen, D. L. and Kurz, M. (1998). The effects of body size and extrinsic mass on the locomotion of the ornate box turtle, *Terrapene ornata*. *J. Herpetol.* **32**, 144-150.
Zani, P. A. and Kram, R. (2008). Low metabolic cost of locomotion in ornate box turtles, *Terrapene ornata*. *J. Exp. Biol.* **211**, 3671-3676.
Zani, P. A., Gottschall, J. S. and Kram, R. (2005). Giant Galápagos tortoises walk without inverted pendulum mechanical-energy exchange. *J. Exp. Biol.* **208**, 1489-1494.
Zug, G. R. (1971). Buoyancy, locomotion, morphology of the pelvic girdle and hindlimb, and systematics of Cryptodiran turtles. *Misc. Pubs. Mus. Zool. Univ. Mich.* **142**, 1-98.

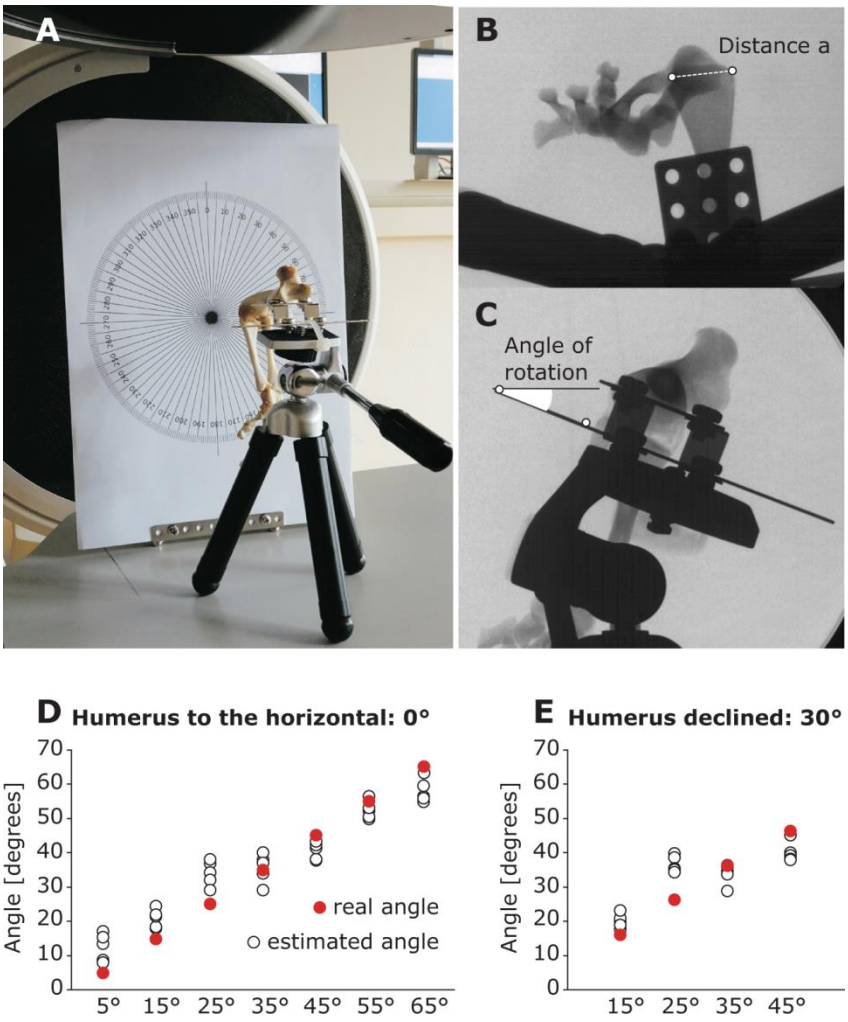

Fig. S1. Measurement accuracy of humerus long axis rotation. (A) The forelimb skeleton of a *Testudo* specimen is mounted on a mini-tripod and placed in front and below the image intensifiers of the C-arm fluoroscope. The platform of the tripod has 3 rotational DOF. We rotated it stepwise and simulated an increasing outwardly-directed long axis rotation of the humerus. We recorded each position in ventrodorsal and frontal perspective. In the first series of steps, the humerus was in parallel to the ground, in a second series we declined the elbow by 30°. (B) The projected distance **a** between the landmarks at the distal condyles was determined from each recording. The measurement of the distance at each position was repeated five times. Maximum distance **c** at 0° rotation was compared to the distance obtained from the skeleton. The measurement error ranged between 0.2 and 1.5 mm and corresponded to the maximum differences among the five measurements obtained at the other platform angulations. (C) The platform angle represents the angle of humerus long axis rotation. (D) Deviation of the estimated angle of rotation from the real angle at the

horizontal position of the humerus. The angle is calculated using the formula: cos α = a/c. In the range of 35° to 55°, the accuracy of measurement depends only on the error of landmark tracking (max. deviation ± 7°). If the cosine of the angle approaches one of the vertices of the cosine wave (0 or 1), a systematic error occurs because of the non-linear wave form. (E) Deviation of the estimated angle of rotation from the real angle at the declined humerus position. The changing orientation of the humerus did not increase the error of landmark tracking significantly. Deviations between estimated and real angle of rotation are similar to those measured at the horizontal humerus position.